


# Towards higher scalability of hybrid optical CDMA network

Ivan Glesk<sup>1</sup>  · Tolulope B. Osadola<sup>1</sup> · Wing C. Kwong<sup>2</sup>

Received: 10 February 2017 / Accepted: 8 July 2017  
© The Author(s) 2017. This article is an open access publication

**Abstract** A novel approach for improving the number of simultaneous users in a hybrid OCDMA-OTDMA network is proposed and analysed. OCDMA system is based on two-dimensional wavelength-hopping time-spreading codes with multi-wavelengths picosecond carriers. The scalability increase was achieved by adding a third dimension to separate OCDMA user groups within OTDMA time slots by assigning them into different wavelength bands. We have shown this will scale-up the system capacity proportionally to the number of assigned wavelength bands. A self-clocking all-optical time gate was then demonstrated as an effective means for suppressing the growing detrimental multi access interference noise resulted from this capacity increase.

**Keywords** OCDMA · OTDMA · All-optical clock recovery · Scalability

## 1 Introduction

Recent advances in information technology have increased the demand for large communications bandwidth (Berthold 1998). Optical code division multiple access (OCDMA) has been widely investigated as a potential alternative to orthogonal frequency division multiple access (OFDMA) (Ergen 2009), wavelength division multiplexing (WDM) (Glesk et al. 2008) and optical time division multiplexing (OTDM) (Hao et al. 2013). Several implementations of incoherent (Glesk et al. 2008) or coherent OCDMA (Amaya et al. 2011) have been reported and investigated in the literature with the ultimate aim of achieving a highly scalable system that is capable of handling large number of simultaneous users without compromising system performance. In particular, the use of

---

✉ Ivan Glesk  
ivan.glesk@strath.ac.uk

<sup>1</sup> EEE Department, University of Strathclyde, 204 George Street, Glasgow G1 1XW, UK

<sup>2</sup> Department of Engineering, Hofstra University, Hempstead, NY 11549, USA

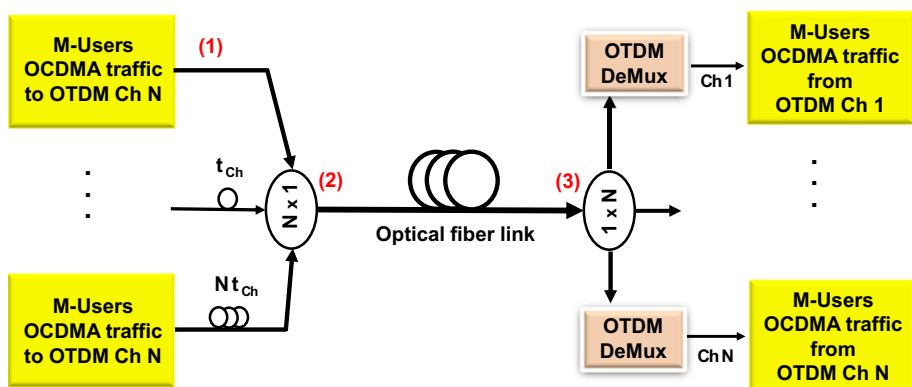
multiplexing (WDM-OCDMA Kitayama et al. 2006, TDM-OCDMA Yoshima 2010) schemes to form hybrid designs are recently being proposed in order to exploit the advantages of each of the individual techniques.

Osadola et al. (2012) proposed and demonstrated a novel architecture for increasing the scalability of an incoherent OCDMA system by employing the technique of OCDMA code reuse that enables different groups of OCDMA users to transmit in separate OTDMA channels. We showed that the scalability of such hybrid system is increased by a factor of  $M \times N$  where  $N$  is the number of OTDM channels and  $M$  is the number of simultaneous OCDMA users per the OTDM channel.

In this paper, we propose and analyze a novel approach that will further increase the scalability of the OCDMA-OTDMA system we originally reported in Osadola et al. 2012. In this new approach, a third dimension is being added to the original OCDMA-OTDMA architecture by allowing multiple OCDMA user groups assigned to different wavelength bands to transmit simultaneously within each OTDM channel. (Note that in general, it is possible to implement coherent or incoherent OCDMA schemes in any channel of the OTDM system). Our analysis and discussions in this paper assumes the use of multi-wavelength two dimensional wavelength-hopping time-spreading (2D-WH/TS) OCDMA codes in all OCDMA sub-systems operating in OTDM channels. Our OCDMA implementation and the overall system performance analysis also reflect using 2D-WH/TS codes based on multiwavelength picosecond pulses (Yang and Kwong 2002). In support of building such system we also demonstrate an all-optical self-clocking method for multi-access interference suppression by using an all-optical time gating technique with a semiconductor optical amplifier -based Mach-Zehnder interferometer (MZI-SOA).

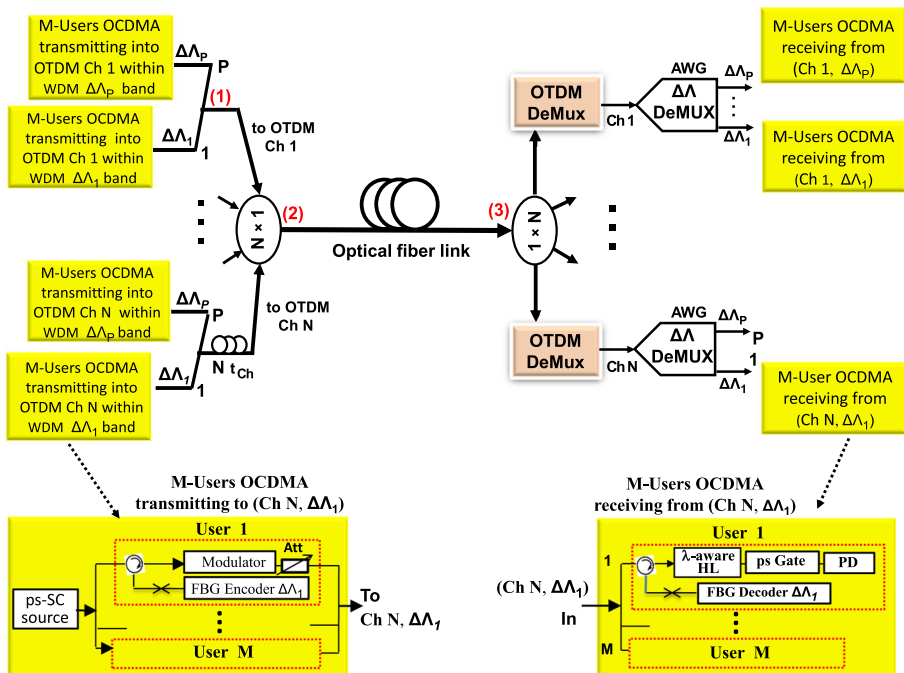
## 2 Design of a highly scalable OCDMA over OTDMA hybrid system

Figure 1 shows our original concept of a hybrid point-to-point broadcast-and-select transmission architecture based on the  $M$ -users OCDMA transmitting over  $N$  channels OTDMA which was described in details in Osadola et al. (2012). As reported, each  $M$ -users OCDMA system uses 2D-WT/TS code set.



**Fig. 1** Block diagram of a Broadcast-and-Select network architecture based on OCDMA over  $N$ -channel OTDMA as reported in Osadola et al. (2012)

Our newly proposed scheme retains the hybrid OCDMA over TDMA approach (Osadola et al. 2012) but introduces a major scalability upgrade to the OCDMA system which broadcasts into individual OTDMA time slots. Because of limitations imposed by higher data rates on the number of available chips and limits imposed by the physical impairments of the fiber used as the transmission medium (Yang and Kwong 2002), it might not be practically feasible to further increase the scalability of single ‘standalone’ 2D-WH/TS OCDMA system beyond the numbers indicated in Osadola et al. (2012). To overcome this scalability bottleneck instead of using the available wavelengths spectrum  $\Lambda$  to form a single 2D-WH/TS code set for supporting just one X-Users OCDMA system (as traditionally done), we are proposing that the available fibre spectrum is divided into  $P$  wavelengths sub-bands  $\Lambda_i = \Lambda/P$ , each supporting one M-Users OCDMA system ( $P$  in total, see (1) in Fig. 2). Each wavelengths sub-band may have either equal bandwidth allocation or, if required, in order to support special type of applications, an unequal allocations. The needed OCDMA code wavelength carriers for 2D-WH/TS OCDMA codes to support the  $P \times M$ -User OCDMA architecture can be generated by slicing the spectrum of an optical supercontinuum of picosecond duration by a fiber Bragg grating (FBG) encoder (Osadola et al. 2012), arrayed waveguide grating (AWG), or thin film filter (TFF) (Glesk et al. 2005). Optical code carriers can also be obtained from a set of multiwavelength laser arrays (Glesk et al. 2008). In this study we assume the use of 2D-WH/TS OCDMA codes generated by fiber Bragg grating (FBG) encoders (Osadola et al. 2012).



**Fig. 2** Block diagram of an upgraded Broadcast-and-Select network architecture based on multi-band OCDMA over N-channel OTDMA. ps-SC—picosecond continuum source, FBG Encoder/Decoder  $\Delta\Lambda_1$ —fiber Bragg grating Encoder/Decoder generating/decoding User 1 2D-WH/TS code in  $\Delta\Lambda_1$  spectral band, Att—optical attenuator, 1xN—power splitter,  $\Delta\Lambda$  DeMUX—wavelength demultiplexer,  $\lambda$ -aware HL—wavelength-aware hard-limiter

**Fig. 3** 2D-WH/TS OCDMA systems each operating within its wavelength bands  $\Delta\Lambda_i$  and transmitting into the OTDM Ch 1

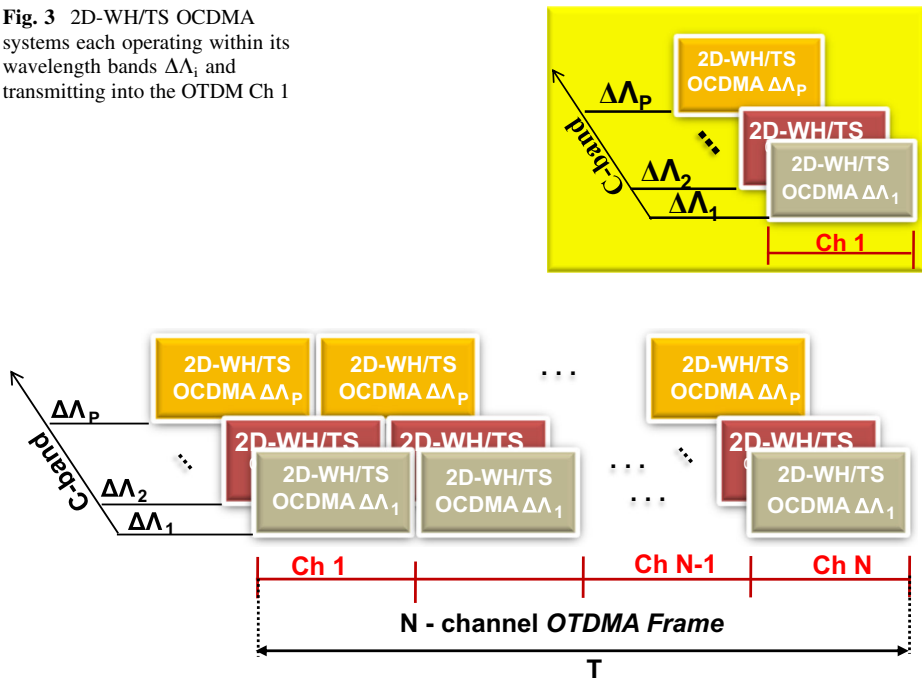


**Fig. 4** N-channel OTDMA frame where each channel contains P groups of M-Users OCDMA

**Data transmission** A detailed architecture of an M-User OCDMA is shown in left-bottom of Fig. 2. Each of P of M-Users OCDMA (for example see (1) in Fig. 2) is a 2D-WH/TS OCDMA system using for data transmission a multiwavelength 2D-WH/TS code-set with a code weight  $w$  from its  $\Delta\Lambda_i$  bandwidth allocation and transmits into OTDMA time slot Ch 1 (see Fig. 3). A C-band spectrum covers 1535 nm to 1565 nm. If this spectrum is divided by following the 200 GHz (0.4 nm) ITU standards, this would allow for about 75 different wavelengths pulses to be allocated for P different 2D-WH/TS code-sets (Yang and Kwong 2002).

Wavelength pulses (OCDMA code carriers) used by any given 2D-WH/TS OCDMA in  $\Delta\Lambda_i$  in Fig. 3 where  $i = (1, 2, \dots, P)$  occupy a wavelength interval  $\Delta\Lambda_i$ . In general,  $\Delta\Lambda_i = \Lambda/w$  where  $\Delta\Lambda_i$  is a wavelength spectrum assigned to the 2D-WH/TS OCDMA sub-system and  $w$  is the number of wavelengths (code carriers) used (the code weight). As a result of this architecture, a P number of M-Users OCDMA  $\Delta\Lambda_i$  can coexist together in the given spectral space  $\Lambda$  without interfering with each other. Please note that different code-sets will not share any wavelength. The resulting traffic from  $P \times M$ -Users OCDMA sub-systems is now time division multiplexed into an OTDM frame. The OTDM channel duration is set not to exceed the longest code-set of any of the M-Users OCDMA (see Fig. 3). The time multiplexing is done using  $N \times 1$  power coupler with an appropriate delay  $N \times t_{Ch}$ , where  $N$  is the OTDMA channel number. The combined resulting OTDM traffic is then launched into a fiber optic transmission link. In case that each group of M-Users OCDMA uses equal bandwidth the number of simultaneous users  $k$  in this new architecture will be  $P \times M$ -Users per OCDMA  $\times$  number of OTDMA channels  $N$ .

Figure 4 shows the resulting generated traffic seen at the point labeled (2) in Fig. 2. Here we can recognize P sets of M-Users OCDMA sub-systems encapsulated a parallel fashion way into N-channel OTDMA frame.

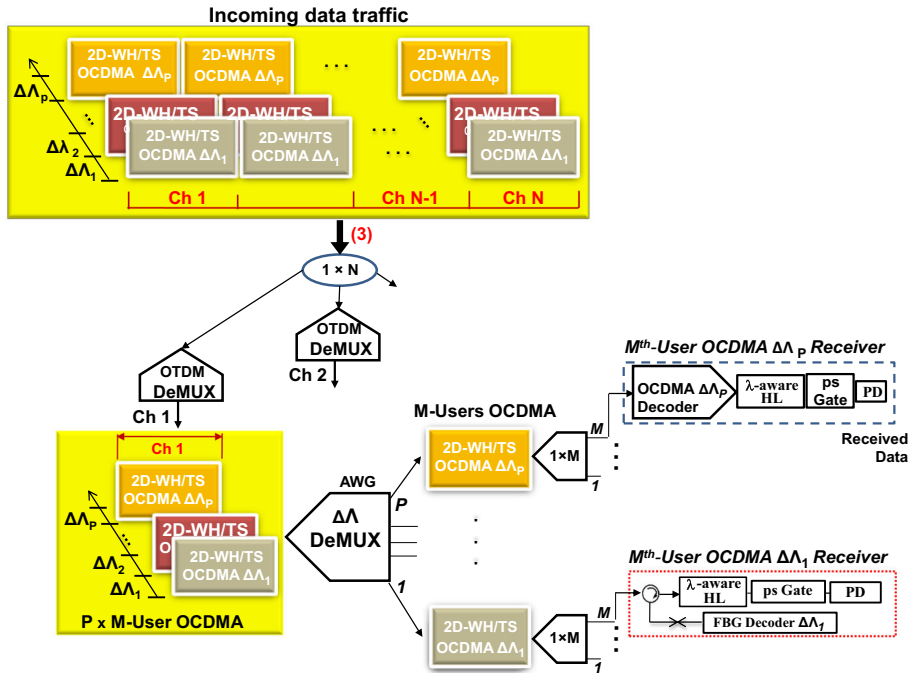


**Fig. 5** Illustration of a data recovery by the User M; ps—picosecond, PD—photodetector, AWG—arrayed waveguide grating, DeMUX—demultiplexer,  $\lambda$ -aware HL— $\lambda$ -aware hard-limiter

Depending on the application, the code-set used by individual OCDMA system groups across different OTDMA time slots can either be the same or can vary to meet the specific application needs. If kept the same, then a hardware reuse will be possible leading to cost savings. As previously stated, the analysis and discussions in this paper will assume the reuse of multi-wavelengths 2D-WH/TS OCDMA code sets in OTDMA time slots.

**Data reception** Figure 5 shows details of User M's data recovery process. At the receiving end (point (3) in Fig. 2) a power splitter  $1 \times N$  is used to divide the incoming data traffic into N outputs. Each output of the  $1 \times N$  splitter is time-demultiplexed by an OTDM DeMUX. This way the content of each OTDMA channel is obtained, i.e., the combine data traffic of  $P \times M$ -Users OCDMA operating in the given OTDMA channel. This OTDM DeMUX operation for example can be performed by using a Mach-Zehnder based demultiplexer. After this, the individual M-Users OCDMA groups are separated from each other by wavelength demultiplexing using  $\Delta\lambda$ -DeMUX - a coarse AWG having its ports bandwidth equal to  $\Delta\lambda_i$ . At this point, at each output port P of the  $\Delta\lambda$ -DeMUX, we now have the data traffic originated from M-Users OCDMA sub-system which were transmitted into  $(\Delta\lambda_i, N)$  'space'. After this, the signal is split M-times by a  $1 \times M$  power splitter and delivered to individual M-Users OCDMA  $\Delta\lambda_i$  receivers to recover the OCDMA auto-correlation (transmitted data). This is done by ensuring the Mth-User OCDMA decoder matches the corresponding Mth-User encoder. To ensure high performance of 2D-WH/TS OCDMA sub-systems the OCDMA receivers are fitted with a wavelength-aware hard-limiter described in (Baby et al. 2004). Related performance improvement is discussed in Sect. 3 (Fig. 6).

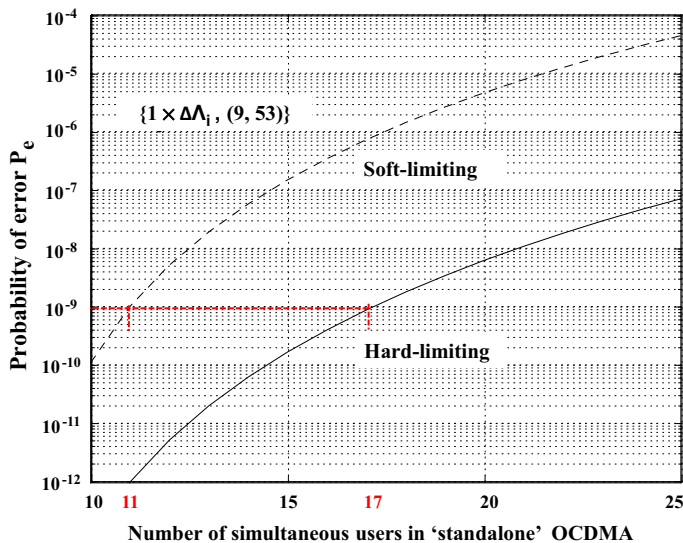


**Fig. 6** System performance of standalone 2D-WH/TS OCDMA with/without hard-limiting receiver

In addition, in Sect. 4, we describe an experimental demonstration of ultra-fast optical time gating to be used in OCDMA receivers for suppressing the multiple access interference that might occur as a result of increased traffic in this highly scalable hybrid system.

### 3 Scalability calculations

We will now calculate the total number of simultaneous users  $k$  this hybrid system can support. First, the  $M$ -Users OCDMA system performance, i.e. the probability of error  $P_e$ , of any of the  $P(w, N_c)$ -2D-WH/TS OCDMA sub-system can be obtained using Eq. (1) (Yang and Kwong 2002, Kwong and Yang 2013).

$$P_e = \frac{1}{2} \sum_{j=0}^{St} (-1)^j \binom{w}{j} \left( 1 - \frac{j q_{1,1}}{w} \right)^{M-1} \quad (1)$$

where  $N_c$  is a number of OCDMA chips,  $w$  is a code weight, and  $q_{1,1}$  is the hit probability given as Osadola et al. (2012)

$$q_{1,1} = \frac{\text{code weight } (w)}{2 \times \text{code length } (N_c)} \quad (2)$$

For an optimum performance,  $St$  is set to be equal to  $w$  (Osadola et al. 2012). It is important to note that Eq. 1 holds for systems where a picosecond sampling of the auto-correlation OCDMA peak has been implemented. Equation 1 is a theoretical equation based on combinatorial analytical model (Yang and Kwong 2002; Kwong and Yang 2013; Azizoglu et al. 1992; Ohtsuki 1997) for any “asynchronous” 1-D and 2-D optical CDMA codes that have the cross-correlation function of at most 1, such as the 2-D carrier-hopping prime codes (Yang and Kwong 2002; Kwong and Yang 2013). “Asynchronous” means that the

codes do not have to be aligned with the time origin. In other words, users can transmit at will, without the need to schedule the transmission timing with other users or globe clock synchronization. It also assumes the use of hard-limiting receiver in front of 2-D decoder or the use of a wavelength-aware hard-limiting receiver (Baby et al. 2004) for reducing the effect of multiple-access interference from the codewords of interfering users. In case of the wavelength-aware hard-limiting receiver implementation, the recovered signal by the user's FBG decoder is examined by the wavelength-aware hard-limiter (Baby et al. 2004) to ensure that all  $w$  wavelength code carriers are present and the recovered signal threshold is  $w$  (each wavelength carrier is present only 'one time'). Only if this is true, the recovered signal is treated as being the user's auto-correlation (i.e., the data signal).

In general, a receiver without the hard-limiter is called a soft-limiting receiver. Although it is more complex to implement, the hard-limiting receiver can lessen the localization of strong interference and equalize the interference effects from simultaneous users of different optical powers or geographical locations (i.e., the near-far problem) (Yang and Kwong 2002; Kwong and Yang 2013). As a result, the hard-limiting receiver would result in better system performance as seen in Fig. 7, in which the hard-limiting probability of error is always lower than the soft-limiting one. In Fig. 7, the 2-D carrier-hopping prime codes (Yang and Kwong 2002; Kwong and Yang 2013) with  $w = 9$  and  $N_c = 53$  are used to compare the hard-limiting probability of error, the  $P_e$  from Eq. (1), and the soft-limiting probability of error, from Eq. (2), as a function of the number of simultaneous users per group  $M$ . For reference, the soft-limiting probability of error  $P_e$  (soft) of the 2-D carrier-hopping prime codes was derived in Yang and Kwong (2002) and Kwong and Yang (2013) as

$$P_e(\text{soft}) = \frac{1}{2} \sum_{j=w}^{M-1} \binom{M-1}{j} (q_{1,1})^j (1 - q_{1,1})^{M-1-j} \quad (2)$$

For example, using the benchmark of  $P_e = 10^{-9}$ , the hard-limiting receiver can support up to  $M = 17$  simultaneous users, while the soft-limiting receiver can only support  $M = 11$  in Fig. 6. Thus, the following numerical study assumes the use of hard-limiting receiver. For

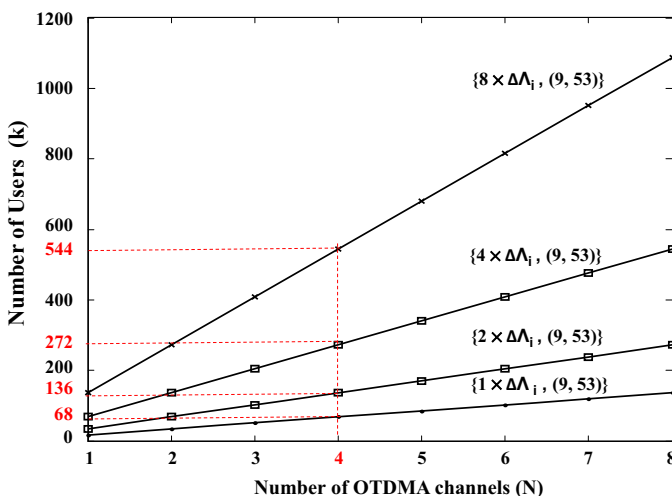


**Fig. 7** System scalability calculations for a hybrid multi band OCDMA over OTDMA

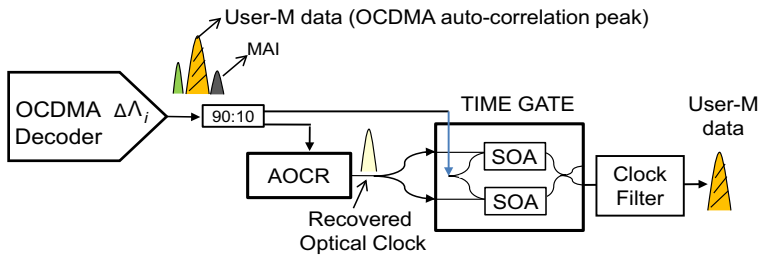
the purpose of the total system scalability calculations cases where  $P = 1$  will be referred to as a 'standalone' M-Users 2D-WH/TS OCDMA defined by parameters  $(w, N_c)$ , in general  $\{P \times \Delta\lambda, (w, N_c)\}$ . From our calculations using Eq. 1 we found that for  $w = 9$ ,  $N_c = 53$  this system will support  $M = 17$  users with  $\text{BER} = 10^{-9}$ . Because codes in all  $P$  WDM  $\Delta\lambda_i$  bands and  $N$  OTDMA time slots are not causing any interference, for a system with  $P = 2$  WDM  $\Delta\lambda$  bands, i.e., two OCDMA groups operating per an OTDMA time slot the number of simultaneous users will increase to  $k = P \times M = 2 \times 17 = 34$ ; the  $\text{BER} = 10^{-9}$  will still be maintained. If such system is now overlaid over a four-channel OTDMA ( $N = 4$ ), it will support up to  $k = 4 \times 34 = 136$  simultaneous users (see Fig. 7) without any deterioration in its performance. Also as seen from Fig. 7, the number of simultaneous users can be scaled up to  $k = 544$  when the number of OCDMA groups  $P$  per OTDM channel is increased to eight. By generalizing the above, the total number of simultaneous user in the proposed system is  $k = N \times P \times M$ . To verify a feasibility of such a system we conducted power budget calculations which included splitting losses, transmission loss over the demonstrated distance, and the losses incurred by individual devices. From these calculations, we found that when a photo-receiver having -30 dBm sensitivity is used as a detector for each individual user, then a 30 dB/10 dBm EDFA can be used to amplify each OCDMA group within the  $\Delta\lambda$  wavelengths band over all four timeslots. Such EDFA will be capable of supporting  $k = 128$  simultaneous users if based on (9,53)-OCDMA over 4-channel OTDMA ( $\text{BER} = 10^{-9}$ , no FEC) or  $k = 256$  simultaneous users based on a (9,53)-OCDMA over 4-channel OTDMA with the FEC implementation.

#### 4 Experimental demonstration of multi access interference suppression by using self-clocked all-optical picosecond gate in the OCDMA decoder

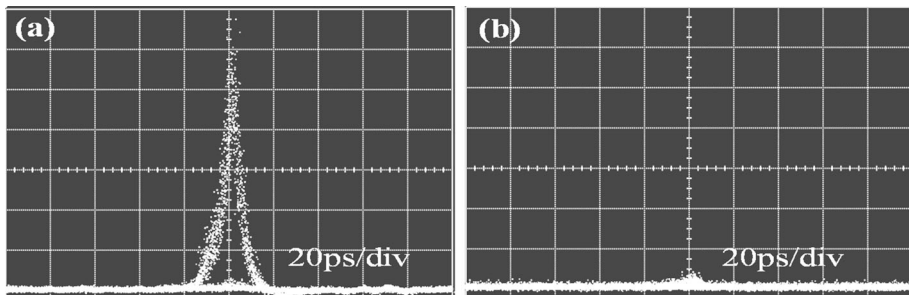
As a result of the increased number of simultaneous users in the described system, multiple access interference (MAI) will be increased thereby resulting in the bit error rate (BER) deterioration. Also, aside the detrimental effects of MAI, at high data rates, the received signal may also suffer from timing jitter. The effect of timing jitter will cause significant problems to achieve receiver synchronization. To achieve a high performance OTDMA, a precise timing control and synchronization will be required. The synchronization can be achieved using a clock signal that is either generated from the incoming signal or by sending a separate clock signal from the transmitter. In order to achieve conditions required for using Eq. 1, sub picosecond sampling of the auto-correlation peak is necessary. Therefore extracting the clock signal from the incoming signal will suppress the timing jitter and provide clock pulses that are 'fast' enough to create the needed sampling window. An all-optical clock recovery from OCDMA signal has been previously demonstrated in Idris et al. (2013a). It was shown that it is possible to extract an optical clock from the auto-correlation output of an OCDMA decoder.

Figure 8 shows a schematic diagram of a self-clocked time gate which uses an all-optically recovered clock as the control signal for a semiconductor optical amplifier (SOA) based Mach-Zehnder interferometric switch (MZI-SOA) which was used as an all-optical time gate. In our experiment a decoded 2D-WH/TS OCDMA signal was fed into the all-optical time gate after passing through a 90/10 optical splitter such that 10% of the signal power was tapped off as an input signal into the clock recovery circuit. The clock signal





**Fig. 8** All-optical time gating using MZI-SOA based time gate. The control signal for the picosecond self-clocked time gate was obtained from the all optical clock recovery circuit (AOCR) (Idris et al. 2013b). SOA—semiconductor optical amplifier, MAI—multi access interference



**Fig. 9** Eye diagram recorded at the output of the MZI-SOA time gate: **a** when the optical clock (control signal) is present; **b** in the absence of the optical clock

generated by the all-optical clock recovery circuit (AOCR) was then fed into the control ports of the MZI-SOA –based all-optical time gate (AOTG) to generate an 8 ps switching window through which the decoded OCDMA auto-correlation signal was gated thus removing the multi-access interference (MAI). The OCDMA signal at 2.4 Gb/s was obtained from the testbed described in (Osadola et al. 2011) which uses 4 wavelengths pulses ( $\lambda_1 = 1551.72$  nm,  $\lambda_2 = 1550.92$  nm,  $\lambda_3 = 1552.52$  nm,  $\lambda_4 = 1550.12$  nm) to form 2D-(4,47) carrier-hopping time-spreading prime codes based on 100 GHz ITU grid positioned in 47 time chips each of 8 ps duration. Figure 9a shows the output signal from the AOTG when the control pulse was present and Fig. 9b shows the output when the control pulse was absent. From the obtained result it was concluded that it is possible to utilize the all-optically recovered clock to control the AOTG. One major advantage of using the recovered clock (self-clocking) is the jitter suppression.

## 5 Conclusions

We have proposed a novel architecture to improve the scalability of the previously demonstrated hybrid OCDMA–OTDMA system (Osadola et al. 2012). To increase a number of simultaneous users, a third dimension was added to the original OCDMA–OTDMA scheme by allowing multiple OCDMA sub-systems to reside in different wavelength bands before being transmitted simultaneously into OTDM time slots (channel). To do these, 2D-WH/Ts codes based on multi-wavelength picosecond pulses are design to occupy P wavelength bands. Each band supports one of the P M-Users OCDMA

systems who then simultaneously operate in a given OTDMA channel. Approach can also support hardware reuse and can therefore offer some cost savings. Our OCDMA-OTDMA system scalability analysis based on  $P = 8$ ,  $N = 4$ ,  $M = 17$  shows that up to 544 users can broadcast simultaneously. (Compare to only 68 simultaneous users in the original hybrid scheme,  $P = 1$ ).

The conducted experiment has confirmed the effectiveness of the all-optical picosecond time gate self-clocking as a means of suppressing the multi access interference noise resulted from the accumulation of timing jitter during transmission that would be detrimental to system performance.

**Acknowledgements** This project has received funding from the European Union's Horizon 2020 research and innovation programme under the Marie Skłodowska-Curie Grant Agreement No. 734331.

**Open Access** This article is distributed under the terms of the Creative Commons Attribution 4.0 International License (<http://creativecommons.org/licenses/by/4.0/>), which permits unrestricted use, distribution, and reproduction in any medium, provided you give appropriate credit to the original author(s) and the source, provide a link to the Creative Commons license, and indicate if changes were made.

## References

- Amaya, W., Pastor, D., Banos, R., Garcia-Munoz, V.: Multi-channel en/decoding devices for WDM - coherent direct sequence OCDMA applications based on super structured fibre Bragg gratings. In: 13th International Conference on Transparent Optical Networks (ICTON 2011), pp. 1–4 (2011)
- Azizoglu, M., Salehi, J.A., Li, Y.: Optical CDMA via temporal codes". IEEE Trans. Commun. **40**(7), 1162–1170 (1992)
- Baby, V., Brès, C.-S., Xu, L., Glesk, I., Prucnal, P.R.: Wavelength aware receiver for enhanced 2D OCDMA system performance. Electron. Lett. **40**(6), 385–387 (2004)
- Berthold, J.: Evolution of WDM in transport networks. Optical Fiber Communication Conference and Exhibit, 1998. (OFC'98 Technical Digest), pp. 13322–13327 (1998)
- Ergen, M.: Mobile Broadband, Including WiMAX and LTE. Springer, New York (2009)
- Glesk, I., Baby, V., Brès, C.-S., Prucnal, P.R., Kwong, W.C.: Design and demonstration of a novel incoherent optical CDMA system. IEEE Military Communications Conference (MILCOM 2005) 5, pp. 3155–3161 (2005)
- Glesk, I., Prucnal, P.R., Andonovic, I.: Incoherent ultrafast OCDMA receiver design with 2 ps all-optical time gate to suppress multiple-access interference. IEEE J. Sel. Top. Quantum Electron. **14**(3), 861–867 (2008)
- Hao, H., Munster, P., Palushani, E., Galili, M., Mulvad, H.C.H., Jeppesen, P., Oxenlowe, L.K.: 640 Gb/s phase-correlated OTDM NRZ-OOK generation and field trial transmission. J. Lightwave Technol. **31**(4), 696–701 (2013)
- Idris, S.K., Osadola, T.B., Glesk, I.: OCDMA receiver with built-in all-optical clock recovery. Electron. Lett. **49**(2), 143–144 (2013a)
- Idris, S.K., Osadola, T.B., Glesk, I.: Towards self-clocked gate OCDMA receiver. J. Eur. Opt. Soc. Rapid. Publ. **8**, 13013 (2013b)
- Kitayama, K., Wang, X., Wada, N.: OCDMA over WDM PON-solution path to gigabit-symmetric FTTH. J. Lightwave Technol. **24**(4), 1654–1662 (2006)
- Kwong, W.C., Yang, G.-C.: Optical Coding Theory with Prime. CRC Press, New York (2013)
- Kwong, W.C., Yang, G.-C., Baby, V., Brès, C.-S., Prucnal, P.R.: Multiple-wavelength optical orthogonal codes under prime-sequence permutations for optical CDMA. IEEE Trans. Commun. **53**(1), 117–123 (2005)
- Lin, Y.-C., Yang, G.-C., Chang, C.-Y., Kwong, W.C.: Construction of optimal 2D optical codes using  $(n, w, 2, 2)$  optical orthogonal codes. IEEE Trans. Commun. **59**(1), 194–200 (2011)
- Ohtsuki, T.: Performance analysis of direct-detection optical asynchronous CDMA systems with double optical hard limiters. J. Lightwave Technol. **15**(3), 452–457 (1997)
- Osadola, T.B., Idris, S.K., Glesk, I., Sasaki, K., Gupta, G.C.: Method for power re-equalization of wavelength pulses inside of OCDMA codes. IEEE J. Quantum Electron. **47**(8), 1053–1058 (2011)

- Osadola, T.B., Idris, S.K., Glesk, I., Kwong, W.C.: Network scaling using OCDMA over OTDM. *IEEE Photon. Technol. Lett.* **24**(5), 395–397 (2012)
- Wang, T.-C., Yang, G.-C., Chang, C.-Y., Kwong, W.C.: A new family of 2D codes for fiber-optic CDMA system with and without the chipsynchronous assumption. *J. Lightwave Technol.* **27**(14), 2612–2620 (2009)
- Yang, G.-C., Kwong, W.C.: *Prime Codes with Applications to CDMA Optical and Wireless Networks*. Artech House, Boston (2002)
- Yoshima, S., Nakagawa, N., Nakagawa, J., Kitayama, K.: 10G-TDM-OCDMA-PON systems. In: 15th Optoelectronics and Communications Conference (OECC 2010), pp. 724–725 (2010)